THE ROLE OF NDT IN THE FRACTURE MECHANICS EVALUATION

L. K. L. Tu* and B. B. Seth**

INTRODUCTION

Fracture mechanics is a powerful technology for evaluating structural reliability. Since the assumption of fracture mechanics is that the flaws with finite sizes exist in the structural components, accurate determination of the initial flaw sizes is therefore very important in the service life prediction. In practice, surface flaws are commonly detected by liquid penetrant, magnetic particle and eddy current examination, whereas the subsurface flaws in large component can only be detected by ultrasonic inspection. The sizes of natural flaws in large components are usually underestimated by ultrasonic testing which can result in a gross overestimation of actual service life by fracture mechanics. It is the objective of this work to (a) illustrate by destructive testing the degree of uncertainty in ultrasonic inspection of natural flaws in large components (b) demonstrate the importance of the accuracy in NDT flaw detectability on the fracture mechanics service life prediction and (c) emphasize the need for more extensive work on NDT/destructive correlation in order to improve the NDT as well as the fracture mechanics reliability.

ULTRASONIC TESTING

In ultrasonic inspection, the flaw size or area is proportional to the intensity of the wave reflected from the flaw, and is also affected by several other factors given below, so that actual flaw size is determined by:

$$\text{Actual flaw area} = C_1\, C_2\, C_3\, C_4\, C_5\, C_6\, C_R\, A_R \qquad (1)$$

where C_1, C_2, C_3, C_4, C_5, C_6 are the corrections for distance, curvature, attenuation, surface roughness, flaw geometry and orientation and other variables, respectively. C_R is the flaw indication as a percentage of the reference distance-amplitude curve. A_R is the area of reference flaw. Experimental data and discussion of these corrections are given in literature [1,2,3].

EXPERIMENTAL

A section of a low alloy steel forging with the dimensions 32 cm O.D. X 10 cm I.D. X 45 cm long was machined to a 3.2 micrometer surface finish. The forging was then ultrasonically examined with a ceramic transducer seach unit with 2.54 cm diameter and operated at 2¼ MHz. The search unit was of the longitudinal wave, faced and internally ground type. SAE 30 oil was used to couple the search unit to forging surface. Cali-

*Advanced Engineer and **Manager, Materials Engineering, Steam Turbine Division, Westinghouse Electric Corp., Phila., PA 19113, U.S.A.

bration of the reflectoscope was done using AISI 4340 steel ultrasonic reference blocks. Several flaws were found near one end of the forging. The relative indication amplitudes of the flaws were obtained from the calibrated distance-amplitude response curve [1].

A thin disc, approximately 5 cm thick, containing ultrasonically detected flaws was saw cut from the forging. X-ray radiographic pictures were taken to locate the flaws in the thin disc. Steel cubes approximately 5 cm in size were further saw cut and ultrasonically c-scanned to provide the three-dimensional flaw shapes and locations. This information is useful in subsequent metallographic sectioning of the flaws. C-scan was performed with a 6.4 mm diameter flat bottom transducer operating at 15 MHz and a 1.3 cm water path. A typical c-scan picture of a flaw is shown in Figure 1. Successive metallographic sectioning and photographing was done at each 0.8 mm depth. Photographs showing the flaw in polished and etched condition at depths of 1.6 mm, 3.2 mm and 9 mm are shown in Figure 2. Three dimensional flaw shape was reconstructed from these pictures.

The chemistry of the inclusion in the flaw was examined by an electron microprobe using energy dispersion spectrum. The results showed that most of the large inclusions found by ultrasonic testing was manganese-sulfides. Some small inclusions rich in calcium, silicon, aluminum and titanium were also found.

RESULTS AND DISCUSSION

Actual Flaw Area

The metallographic sectioning of the steel cubes was made perpendicular to the ultrasonic beam. The flaw area normal to the beam was reconstructed from metallographic sectioning and measured by a planimeter, Figure 3. The flaw was elongated in the axial direction of the forging. The flaw area (A_i) was obtained as a sum of closely located flaws in the steel cube:

$$(A_i) = 12.9 \text{ mm}^2$$

Flaw Area Based on UT Estimation

Using the notations in (1) the flaw area detected by UT is obtained as follows:

$$(A_{NDT}) = C_1\ C_2\ C_3\ C_4\ C_5\ C_6\ (C_R)\ A_R$$

$$= (1)\ (7.2)\ (1)\ (1)\ C_5\ C_6\ (0.2)\ (1.94)$$

$$= (2.80)\ C_5\ C_6$$

where
- C_1 = 1, for using the experimentally corrected distance-amplitude curve [1]
- C_2 = 7.2, for a forging diameter of 32 cm [1,3]
- C_3 = 1, [1,2]
- C_4 = 1, Since forging and calibration blocks have the same 3.2 micrometer surface finish [1,2]

(C_R) = 0.20, [1]

Comparing this with the area found from destructive testing, we have $(A_i)/(A_{NDT}) = C_5\ C_6 = 4.6$. The actual flaw area is therefore significantly larger than predicted from ultrasonic amplitude.

Fracture Mechanics Analysis

Since large voids with rough surfaces were found in our metallographic destructive sectioning in the steel forging, we cannot treat these voids as round edge inclusions. Analytical solutions for cracks eminating from a hole [4-7] indicates that for mode I crack opening the stress intensity factor at the crack tip becomes larger as the crack length becomes shorter as compared to the hole diameter. That is, the voids with short cracks eminating outward or sharp surface irregularities are as dangerous as long cracks. Therefore, these voids were treated as cracks in the fracture mechanics calculation.

Fracture mechanics has been successfully applied to structural reliability evaluation. The critical crack size, a_{cr}, which will cause brittle fracture is calculated by: [8]

$$a_{cr} = (1/M)\ (K_{Ic}/\sigma)^2 \qquad (2)$$

Where:
- M = component geometry parameter = π/Q, for internal crack [8]
  = $1.21\pi/Q$, for surface crack
- Q = $\Phi^2 - 0.212\ (\sigma/\sigma_Y)^2$ = flaw shape parameter [8]
- 2a,2c = depth and length of an internal crack, respectively

The crack growth rate under cyclic loading can be correlated by an empirical equation [9]

$$\frac{da}{dN} = C_o \Delta K^n \qquad (3)$$

Where:
- C_o = constant which takes into account the various environmental and other minor effects
- n = slope of the log da/dN vs. logΔK curve

The number of cycles to propagate certain sizes of cracks to critical sizes can be estimated by integration of the above fatigue crack growth equation.

$$N = \frac{2}{(n-2)\ C_o M^{n/2} \Delta\sigma^n} \left[a_i^{\frac{2-n}{2}} - a_{cr}^{\frac{2-n}{2}} \right], \text{ for } n \neq 2 \qquad (4)$$

and

$$N = \frac{2}{C_o M \Delta\sigma^2} \ln \frac{a_{cr}}{a_i}, \text{ for } n = 2 \qquad (5)$$

Where
- N = number of cycles to failure
- a_i = initial flaw size

Since initial flaw size a_i affects the life N (Equations (4) and (5)), uncertainty in a_i will result in corresponding uncertainty in N. To examine the effect of flaw size underestimated by ultrasonic testing discussed above, the following simplified assumptions were made:

a) Irregular shape flaw can be represented by an ellipse of equivalent area
b) Using actual size a_i and area A_i of the flaw, the equivalent length 2c and ratio of a/2c can be calculated.

Let $a/2c = R$, then $A = \pi ac = a^2 \pi/2R$ or $a_i/a_{NDT} = (A_i/A_{NDT})^{1/2}$. Therefore, the uncertainty in flaw size (a_i/a_{NDT}) measured by NDT is 2.14. Similarly we can calculate a_{NDT} and $a_{NDT}/2c_{NDT}$. The results of all measurements and calculations are summarized in Table 1. The fatigue crack growth equation has been determined experimentally for the low alloy steel used in this study at room temperature in air:

$$\frac{da}{dN} = 4.6 \times 10^{-9} \Delta k^{2.2} \qquad (6)$$

σ_y = 90 ksi (620.5 MPa) and K_{IC} = 45 ksi - in.$^{1/2}$ (49.4 MPa - m$^{1/2}$) for lower shelf.

For a given applied stress and material property, the number of cycles required to propagate an existing initial flaw a_i to a critical size can be calculated from equations 4 and 6.

Since NDT underestimated the flaw size in this test program, the calculated number of cycles (N_{NDT}) to propagate a smaller initial flaw predicted by NDT (a_{NDT}) to a critical size (a_{cr}) is larger than (N_i) required by an actual initial flaw. Using the experimentally determined flaw size, underestimation of flaw size by 2.14 x resulted in an overestimation in cyclic life by 40% in this case. It was assumed that $\sigma/\sigma_y = 0.5$ in the calculation.

Curves of a_i/a_{NDT} vs. N_{NDT}/N_i calculated for $N_i = 10^3$ are shown in Figure 4. For an underestimation of flaw size 2.1 (a_i/a_{NDT}) an overestimation of service life N_{NDT}/N_i of 30 x will result for $\sigma/\sigma_y = 0.5$, $N_i = 10^3$ cycles and a/2c = 0.5. Keeping other variables constant, the overestimation increases with shorter service life N_i, larger a/2c and smaller σ/σ_y ratio. Therefore, uncertainty in detecting flaw sizes can result in large uncertainty in service life calculated by fracture mechanics. The importance of accurate NDT detection of flaws is demonstrated.

CONCLUSION

To improve the reliability of service life prediction, a better NDT/destructive correlation on natural flaws is required. The effect of actual versus NDT detected flaw sizes on cyclic life prediction using fracture mechanics analysis has been demonstrated.

REFERENCES

1. TU, L. K. L. and SETH, B. B., Submitted for publication.
2. KRAUTKRÄMER, J. and KRAUTKRÄMER, H., "Ultrasonic Testing of Materials", Springer-Verlog, New York, Heidelberg, Berlin, 1969.
3. YING, A. S. C., ASME Paper 62-WA-175.

4. TADA, H., PARIS, P. C. and IRWIN, G. R., "The Stress Analysis of Cracks Handbook", Del Res. Corp., Hellertown, Pa., 1973.
5. BOWIE, O. L., J. Math. and Phy., 35, 1956, 60.
6. SIH, G. C., Trans. ASME, J. Appl. Mech., 32, 1965, 51.
7. NEWMAN, J. C., Jr., NASA TND-6376, Aug. 1971.
8. TIFFANY, C. F. and MASTER, J. N., ASTM, STP 381, 1965, 249.
9. JOHNSON, H. H. and PARIS, P. C., Eng. Fract. Mech. 1, 1968, 3.

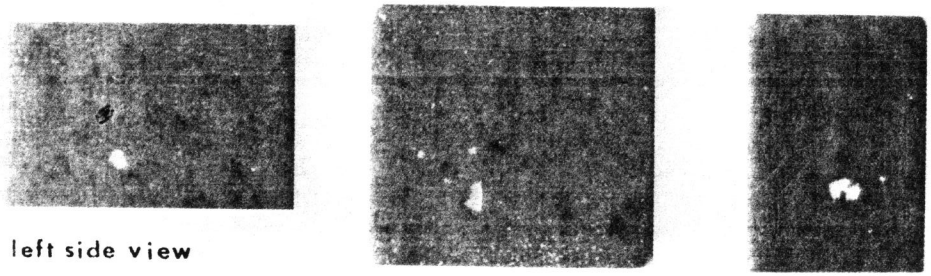

Figure 1 Typical C-Scan Pictures of a Flaw (1.5X)

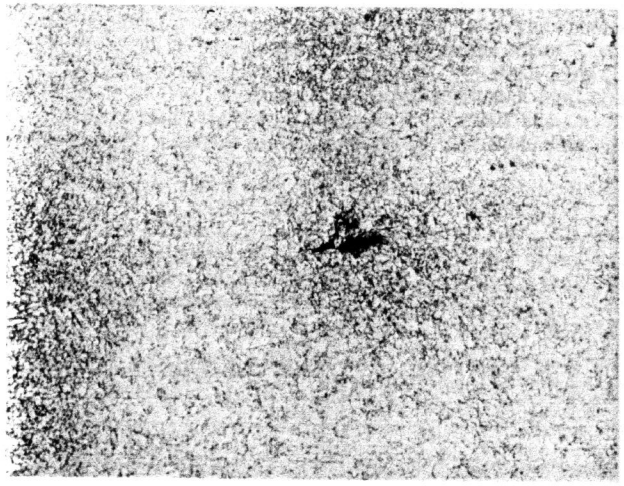

Figure 2(a) Flaw in Steel Cube, Polished and Etched (50X)

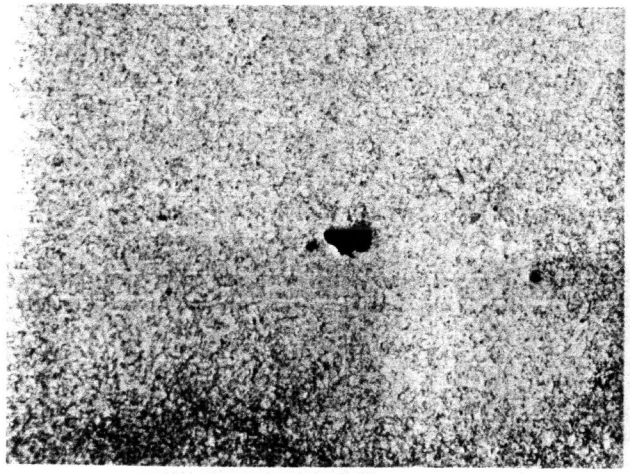

Figure 2(b) Flaw in Steel Cube, 1.6 mm Below Surface (Etched) (50X)

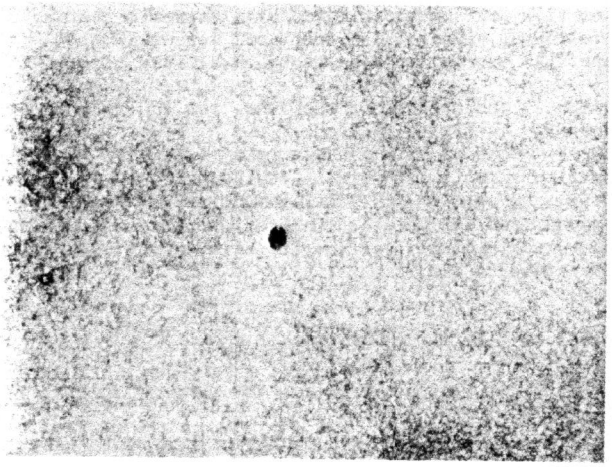

Figure 2(c) Flaw in Steel Cube, 3.2 mm Below Surface (Etched) (50X)

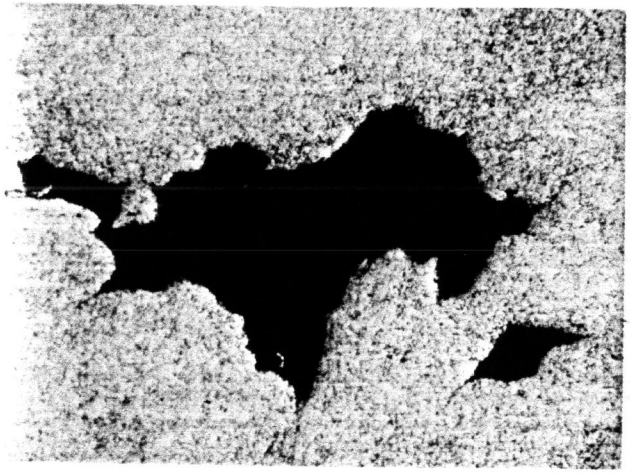

Figure 2(d) Flaw in Steel Cube, 9 mm Below Surface (Etched) (50X)

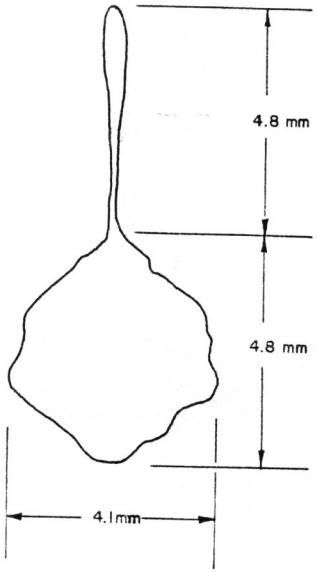

Figure 3 Reconstructed Flaw Area (Perpendicular to the Ultrasonic Beam)

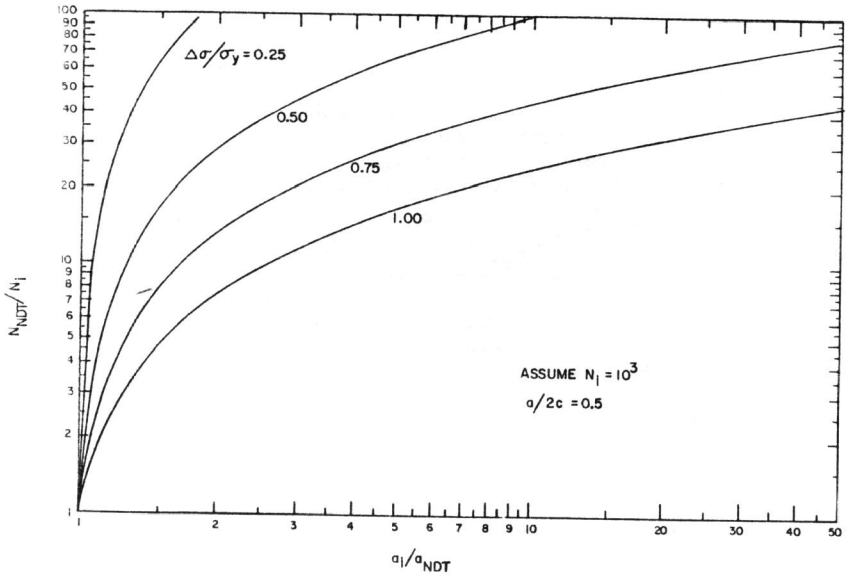

Figure 4a Effect of Uncertainty in NDT on Overestimation of Cyclic Life

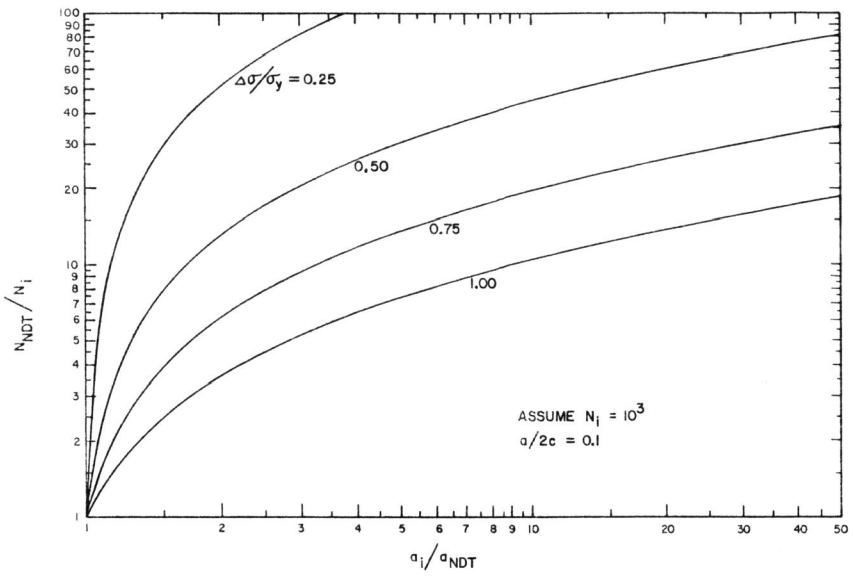

Figure 4b Effect of Uncertainty in NDT on Overestimation of Cyclic Life

Table 1

A_i (mm^2)	A_{NDT} (mm^2)	A_i/A_{NDT}	a_i (mm)	$a_i/a_{NDT} = (A_i/A_{NDT})^{1/2}$	a_{NDT} (mm)	$a_i/2c_i = a_{NDT}/2c_{NDT}$
12.9	2.8	4.6	2.03	2.14	0.95	0.50